Influence of Entrapped Air Pockets on Hydraulic Transients in Water Pipelines

Ling Zhou[1]; Deyou Liu[2]; Bryan Karney, M.ASCE[3]; and Qinfen Zhang, Ph.D.[4]

Abstract: The pressure variations associated with a filling undulating pipeline containing an entrapped air pocket are investigated both experimentally and numerically. The influence of entrapped air on abnormal transient pressures is often ambiguous because the compressibility of the air pocket permits the liquid flow to accelerate but also partly cushions the system, with the balance of these tendencies being associated with the initial void fraction of the air pocket. Earlier experimental research involved systems with an initial void fraction greater than 5.8%; this paper focuses on initial void fractions ranging from 0 to 10% to more completely characterize the transient response. Experimental results show that the maximum pressure increases and then decreases as the initial void fraction decreases. A simplified model is developed by neglecting the liquid inertia and energy loss of a short water column near the air-water interface. Comparisons of the calculated and observed results show that the model is able to accurately predict peak pressures as a function of void fraction and filling conditions. Rigid water column models, however, perform poorly with small void fractions. **DOI: 10.1061/(ASCE)HY.1943-7900.0000460.**

CE Database subject headings: Hydraulic transients; Water pipelines; Pressurized flow; Experimentation; Air entrainment; Oscillations.

Author keywords: Hydraulic transients; Water pipelines; Pressurized flow; experimentation; Air entrainment; Oscillations.

Introduction

A pipe system is the crucial component of many commercial and industrial facilities, including hydropower plants, pump stations, thermal power plants, nuclear power stations, and urban supply and drainage systems. When flow in such a system is initiated, or whenever there is a transition from open channel flow to surcharged flow, the phenomenon of a water column striking an entrapped air pocket could occur. The existence of the entrapped air pocket may lead to unexpectedly high pressures, which can easily result in permanent deformation or even rupture of the pipe (EHG 1996; Guo and Song 1990; Wylie and Streeter 1993).

In the context of filling a pipe system, many researchers have studied the effects of the location and volume of an entrapped air pocket, the water column length, and the size of the orifice at the end of pipe on the peak transient pressure (Cabrera et al. 1992; De Martino et al. 2008; Lee 2005; Lee and Martin 1999; Liu and Suo 2004; Liu and Zhou 2009; Zhou et al. 2011; Martin 1976; Ocasio 1976; Zhou 2000; Zhou et al. 2002). Martin (1976) points out that the most dangerous case is when the air pocket is fully entrapped by surrounding water columns without air release, a situation that could result in high and destructive pressures. Ocasio (1976) conducted a set of experiments in which an air pocket was located between the dead end and a closed valve and demonstrated that the presence of the entrapped air, under conditions of instantaneous valve opening, could lead to extreme surges. He also found that as initial air volume increased, the maximum pressure surge decreased. Zhou (2000) and Zhou et al. (2002) presented experimental measurements from a horizontal pipeline in which the pipe length was constant, the inlet pressure was more than twice the atmospheric pressure and the initial void fractions varied between 20, 50, and 95.2%. This work shows that when less air was present, the maximum pressure of the air pocket increased as the cushioning effect of the air pocket decreased. Lee and Martin (1999) and Lee (2005) investigated the effect of initial void fraction of air pockets in horizontal pipelines with a closed end. They found that, for initial void fractions between 5.8 and 44.8%, smaller initial void fractions resulted in larger maximum pressures for cases with a constant initial water column length and an inlet pressure more than twice the atmospheric pressure.

The previously described studies suggest that the initial void fraction of the air pocket plays a key role in determining peak pressures; however, these studies concern relatively large air pockets and high inlet pressures. To further investigate this phenomenon, an experimental investigation has been conducted on transient flow while filling an undulated pipeline containing a relatively small air pocket under low inlet pressures. The effects of the air pocket on the system pressure are observed, in which the air pocket is entrapped at the dead end of a pipeline. An improved elastic model from the complete elastic water model is introduced to avoid interpolations, and the opening valve time and elevation change of pipe are also considered. The accuracy of the improved model is analyzed and compared to the existing complete elastic water model (Lee's elastic model). Moreover, comparisons of the proposed model to the experiment results are provided.

[1]Ph.D. candidate, College of Water Conservancy & Hydropower Engineering, Hohai Univ., 1 Xikang Rd., Nanjing, China 210098 (corresponding author). E-mail: zlhhu@163.com

[2]Professor, College of Water Conservancy & Hydropower Engineering, Hohai Univ., 1 Xikang Rd., Nanjing, China 210098. E-mail: Liudyhhuc@163.com

[3]Professor, Dept. of Civil Engineering, Univ. of Toronto, 35 St. George St., Toronto, ON, Canada M5S 1A4. E-mail: karney@ecf.utoronto.ca

[4]R&D Associate, Oak Ridge National Laboratory, 1 Bethel Valley Rd., P.O. Box 2008, Oak Ridge, TN 37831-6038. E-mail: zhangq1@ornl.gov

Note. This manuscript was submitted on October 27, 2010; approved on May 18, 2011; published online on May 20, 2011. Discussion period open until May 1, 2012; separate discussions must be submitted for individual papers. This technical note is part of the ***Journal of Hydraulic Engineering***, Vol. 137, No. 12, December 1, 2011. ©ASCE, ISSN 0733-9429/2011/12-1686–1692/$25.00.

Mathematical Model

Fig. 1 shows the configuration of the pipe system envisioned in this work, which consists of a source reservoir, an upstream water column, a valve, and a downstream water column with an entrapped air pocket and an air-water interface. H_r is the upstream (gauge) head and H_u is the corresponding absolute piezometic head. In Fig. 1, L_{11}, L_{12}, and L_{13} are the three identified pipe lengths upstream of the valve, and L_{21}, L_{22}, and L_{23} are the three identified pipe lengths downstream of the valve; D is the pipe diameter and is constant for all sections; V_{a0} and H_{a0} are the initial volume and absolute pressure head (in meters) at the air pocket, respectively; Z_C is the elevation of pipe centerline at the air-water interface. The initial void fraction of the air pocket, α, is the initial air volume to total volume of air and water.

The following assumptions are made in the development of the one-dimensional mathematical model (Cabrera et al. 1992; Zhou et al. 2002):

1. The air pocket occupies the entire cross section;
2. The air-water interface is perpendicular to the centerline of pipe (i.e., the air pocket remains cylindrical in shape);
3. During the filling process, both the dissolution and release of air are negligible;
4. The pipeline is fully closed and no water and air are leaked or released;
5. The wall friction factor for steady flow is applicable under unsteady flow condition;
6. A polytropic law is applicable for the air phase and the polytropic exponent m is constant; and
7. The inertia of air pocket is negligible, and thus the constant pressure is throughout within the air pocket.

Governing Equations

Applying the mass conservation and momentum equations to the water phase in the pipe results in the standard governing equations for water hammer

$$\frac{\partial H}{\partial t}+\frac{a^2}{gA}\frac{\partial Q}{\partial x}=0 \tag{1}$$

$$g\frac{\partial H}{\partial x}+\frac{1}{A}\frac{\partial Q}{\partial t}+\frac{f}{2DA^2}Q|Q|=0 \tag{2}$$

where t = time; x = distance; H = head; Q = discharge; a = wave speed; f = wall friction; A = pipe's cross-sectional area; and g = gravitational acceleration (9.81 m/s^2).

For the solution as a whole, the standard method of characteristics (MOC) is employed to analyze the transient flow in the filling pipe containing an entrapped air pocket (Wylie and Streeter 1993; Lee and Martin 1999; Lee 2005). Compared to a complete elastic water model, a simpler model for the water column is proposed.

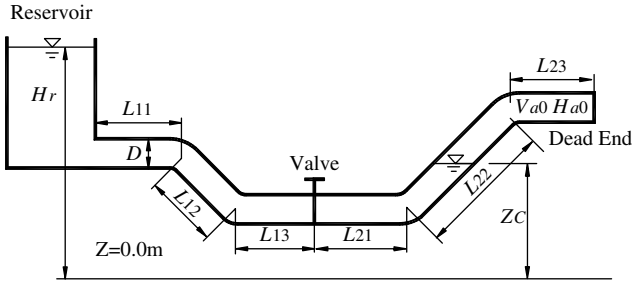

Fig. 1. Defining sketch for theoretical analysis

The governing equations of the water phase are solved with the MOC, but the changes of both the head and flow rate of a tiny water column near the air-water interface are neglected to more conveniently track the air-water interface. The computational system includes the water, air pocket, and air-water interface parts.

Control Equations for Water Phase

The upstream boundary condition, taking into account of the minor loss at the inlet, H_p can be calculated by

$$H_P=H_u-\frac{Q_P^2}{2gA^2}-\xi_j\frac{Q_P|Q_P|}{2gA^2} \tag{3}$$

where ξ_j = minor loss coefficient of the inlet; for positive flow, $\xi_j=0.5$; for negative flow, $\xi_j=1$. The standard orifice equation is used to represent the valve boundary condition (Wylie and Streeter 1993).

Governing Equation for Air Phase

The governing equation for the confined air pocket is

$$H_aV_a^m=H_{a0}V_{a0}^m \quad \text{or} \quad H_aL_a^m=H_{a0}L_{a0}^m \tag{4}$$

where H_a, V_a, and L_a = instantaneous absolute pressure, volume, and length, respectively, of the entrapped air pocket at time t; L_{a0} = initial length of the air pocket before the valve is opened; and m = polytropic exponent. Fast transient phenomena are often assumed to be adiabatic processes with $m=1.4$. Moreover, Zhou (2000) and Lee (2005) demonstrated that the first peak pressure of an entrapped air pocket in a rapidly filling horizontal pipe is better predicted with a polytropic compression exponent $m=1.4$ rather than with $m=1.2$ and $m=1.0$. Therefore, for the relative small air pocket volume and the fast response of the system to the first pressure peak, a polytropic exponent of $m=1.4$ was employed.

Tracking the Air-Water Interface

One of the most challenging aspects of the simulation is that the air-water interface moves with time. Directly applying the MOC to solve the moving interface boundary tends to create interpolation problems. To circumvent this challenge, a key assumption is made: that the liquid inertia and energy loss of a tiny water column ΔLw_i adjacent to the air-water interface can be ignored (namely, the head and water flow rate are both constant throughout the water column of ΔLw_i). The ΔLw_i is continually changed by the movement of the air-water interface, but the length extent of ΔLw_i is related to the MOC grid length. As shown in Fig. 2, as long as ΔLw_i is sufficiently small, this model will generate nearly the same calculated numerical results as the complete elastic water model, while avoiding interpolations. However, an infinitesimal ΔLw_i will lead to running mistakes in the simulation program. Therefore, a rational length extent of ΔLw_i is crucial to ensure the calculated accuracy and realization of the numerical model, and $0.5\Delta x \le \Delta Lw_i < 1.5\Delta x$ is adopted here.

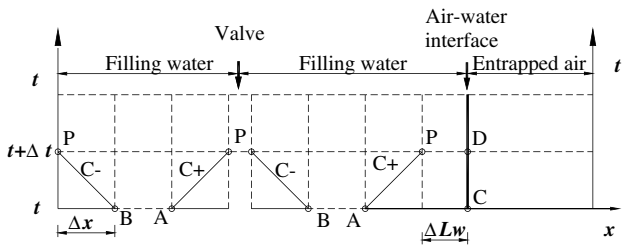

Fig. 2. Definition sketch in x-t plane with fixed grid

J. Hydraul. Eng. 2011.137:1686-1692.

As shown in Fig. 2, C and D are locations of the air-water interface at the known time t and to be determined at $t + \Delta t$. During the calculation, the grid step Δx and Δt are constant, but the movement of air-water interface causes the ΔLw_i change. Consequently, solving ΔLw_i is the key to tracking the interface boundary.

Governing Equation of Air-Water Interface

With an undulating profile, considering the elevation change of the air-water interface, the continuity equation and momentum equation can be written as

$$\frac{dV_a}{dt} = -Q \quad \text{or} \quad \frac{dx_w}{dt} = \frac{Q}{A} \tag{5}$$

$$H_D = H_a + Z_C(x_D) \tag{6}$$

where x_w = distance of the air-water interface from the upstream reservoir; Q = water flow rate at the air-water interface; x_D and H_D = distance and head of the interface at $t + \Delta t$, respectively; Z_c = continuity function of x_D, and when the profile of pipe system is given, the relation between Z_c and x_D is also known.

Tracking the moving boundary allows the location of the air-water interface to be known at any time, and integration of Eq. (5) can be expressed as

$$\int_C^D dx_w = \frac{1}{A}\int_t^{r+\Delta t} Q(t)dt \tag{7}$$

Applying the mean value theorem of integrals and the method of mean function in Eq. (7), the equation can be approximated as

$$x_D = x_C + \Delta t \times \frac{(Q_C + Q_D)}{2A} \tag{8}$$

which defines the new location of the moving boundary, and where Q_C and Q_D = flow rate at points C and D, respectively; and other new terms are defined in Fig. 2.

According to the preceding assumption, the inertia and energy loss of ΔLw_i are ignored. The continuity equation and momentum equation are

$$H_P = H_D \quad \text{and} \quad Q_P = Q_D \tag{9}$$

The proposed analytical model is made up of Eqs. (1)–(9).

Numerical Solution

Fig. 2 shows the computational grid used in solving the governing equations. In this model, the time step Δt and the grid step Δx are both constant during the simulation, and $0.5\Delta x \le \Delta Lw_i < 1.5\Delta x$. By taking account of the valve opening, the solution schemes change with the water length behind the valve (the distance L_{va} is between the valve and the air-water interface). The primary differences can be numerically associated with the solution of the valve:

1. When $L_{va} \ge 1.5\Delta x$, the flow rate and pressure head at the upstream inlet can be computed by combining Eq. (3) and the C^- characteristic equation. The internal nodes can be calculated with the MOC. The flow rate and pressure head at the valve can be obtained through the orifice equation for the valve. During the calculation of the interface boundary, combining characteristic C^+ and Eqs. (4)–(9), the Newton method is employed to solve H_D, Q_D, and x_D. The pressure of the entrapped air pocket, H_a, can be obtained through the gas law.
2. When $0 \le L_{va} < 0.5\Delta x$, it no longer meets the condition $0.5\Delta x \le \Delta Lw_i < 1.5\Delta x$. Now, the upstream inlet and the internal nodes of water part can be computed by using the same method as in the first scenario. However, the calculation at the valve and interface boundary needs to be carried out by combining characteristic C^+, the orifice equation for the valve, and Eqs. (4)–(9). This case is rare and only occurs at the beginning of the valve movement when the pipe upstream of the valve is initially full of water and the pipe downstream of the valve is initially empty or partly filled with a small amount of water (in this paper, the case with air passing through the valve is not considered).

The boundary and initial conditions are: (1) the upstream reservoir head remains constant throughout the simulation; (2) the initial pressure head of the entrapped air pocket is assumed to be atmospheric; (3) the initial flow rate of the water is assumed to be zero to be consistent with the experimental tests conducted (although the model is not limited to this situation); (4) the initial length of the air pocket can be converted from the same air volume based on the basic assumptions of the model; (5) the initial dimensionless valve opening is assumed to be a small value (0.05 is used here) to ensure that the simulation program runs smoothly, and the full valve opening is 1.0.

During the calculation of the water filling process, because of the compression and expansion of the air pocket, conditions of $1.5\Delta x \le \Delta Lw_i$ or $\Delta Lw_i < 0.5\Delta x$ may occur. To validate the assumption of $0.5\Delta x \le \Delta Lw_i < 1.5\Delta x$, it is necessary to add or delete a computed node and the variables at the newly added node must be estimated by interpolation between the nearby nodes.

Experimental Studies

The experiment investigates the effects of the initial void fraction of the entrapped air pocket on the pressure of a filling pipeline system, focusing on cases with relatively small initial void fractions within an undulated pipeline.

Experiment Program

The experiments were conducted at the Hydraulic Laboratory of Hohai University using the experimental apparatus depicted in Fig. 3. The system consists of an upstream reservoir with 5 m^2 cross section, a gate valve, a quarter-turn ball valve, a water vent, and a 4.4445-m-long pipeline with a 9 cm internal diameter and 0.5 cm pipe wall thickness. The pipeline contains five parts: a 125-cm-long horizontal pipe (Pipe 1), a 73-cm-long vertical pipe (Pipe 2), a 121.45-cm-long horizontal pipe (Pipe 3), a 100-cm-long vertical pipe (Pipe 4), and a 25-cm-long horizontal pipe (Pipe 5). The horizontal Pipe 1 with the gate valve is made of PVC and the remaining undulated pipeline is made of transparent organic glass. In the experiments, the air pocket is entrapped at the dead end of the pipeline system. The water vent at the bottom horizontal Pipe 3 and

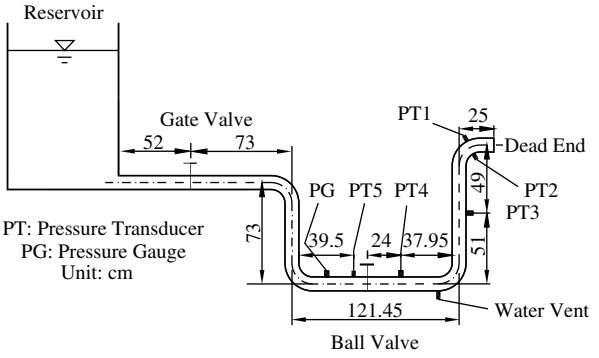

Fig. 3. Diagram of experimental apparatus

J. Hydraul. Eng. 2011.137:1686-1692.

a valve at the dead end of Pipe 5 are used to regulate the initial location of the entrapped air pocket. Initially, the gate valve is fully opened, the ball valve is closed, the air pocket is entrapped at the downstream end, and the water vent is closed.

The measuring system consists of one pressure gauge and five pressure transducers. The pressure gauge is installed immediately upstream of the ball valve to measure the initial static pressure from which the inlet pressure head at the upstream reservoir can also be obtained. The locations of 5 pressure transducers are shown in Fig. 3: PT1 is located near the dead end in the air pocket and thus effectively measures the varying pressure within the air pocket, PT2 is installed at the lower part of the elbow near the dead end, PT3 is at the middle of the vertical pipe (Pipe 4), and PT4 and PT5 are fixed along the lower horizontal pipe (Pipe 3) at 24 cm downstream of the ball valve and 10 cm upstream of the ball valve, respectively. These 5 pressure transducers have the same scale, that is, the fluid pressure scale is from −0.1 to 2.0 MPa; response frequency ranges from 30 to 300 kHz; operating temperatures are permitted within the range of −40 and 150ºC; linearity ranges from 0.03 to 0.3% of the full range; lag error is between 0.03 and 0.3% of the full range. Each of these transducers was calibrated in advance of the tests. During the measurement, the transducers collect at 1,000 Hz. Each of these transducers is connected to a carrier demodulator that is, in turn, connected to a data acquisition board controlled by a personal computer. The data acquisition software is set to automatically initiate data collection. The pressure oscillation history at each of these transducers is displayed on the computer screen and then saved to a file for later analysis.

To facilitate later calibration of the model, the friction factor f of the pipe and the minor loss coefficient for the valves and the pipe elbow are indirectly measured under steady flow conditions. The local loss coefficient for the fully open ball valve is first measured in the range of from 0.1 to 0.13. The friction factor, f, is determined based on total losses, ranging between 0.045 and 0.05, and $f = 0.05$ is adopted in the reported calculations.

Pipe filling is achieved by manually turning the quarter-turn ball valve, so instantaneous valve opening is an ideal condition. The record of a high-speed digital camera shows that the valve opening time (from fully closed to fully opened) ranges from 0.05 to 0.1 s; a valve opening time of 0.1 s is assumed in subsequent calculations.

The speed of the water hammer wave speed is necessary for the MOC solution. The wave speed is measured under the rapid valve closure tests with no air. The wave speed of PVC and organic glass piping filled with water is 400 m/s.

Experimental Results

Assuming that the centerline of the horizontal pipe (Pipe 5) is the datum line, $Z = 0$. The absolute piezometric head at the inlet, H_u is between 14.70 and 16.63 m (correspondingly, H_r is from 4.37 to 6.30 m). The initial elevation of the air-water interface, Z_C, ranges from −0.15 to +0.045 m. The total volume of water and air, and initial air volume can be read from the three-dimensional schematic of the experimental system, which is drawn by using computer-aided design (CAD) software. Correspondingly, the initial void fraction of the entrapped air pocket varies from 0 to 8.02%.

Fig. 4 shows the piezometric head oscillation patterns recorded by the Transducers 1, 2, and 5 (absolute head), with different void fractions for the entrapped air pocket. Comparing the head at the different transducers, it is found that the head at PT2 is always basically close to the head at PT1. This is because both transducers are located in the active area of the air pocket. When the initial void fraction of air pocket is 6.18%, because the air cushioning effect is basically negligible and the water impact force is dominant, the maximum head at PT1 and PT2 are both larger than at PT5, which

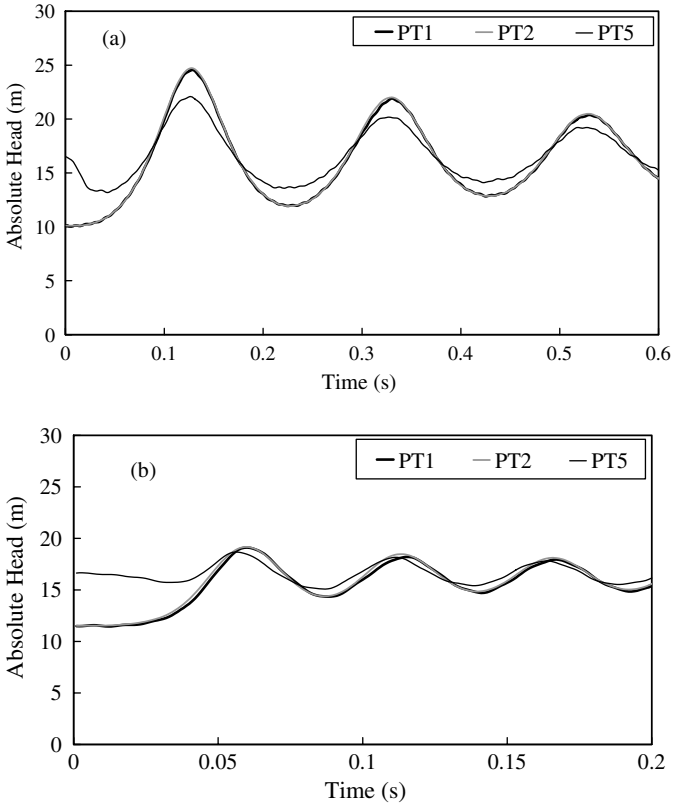

Fig. 4. Head at transducers: (a) $H_u = 16.53$ m, void fraction of air pocket $\alpha = 6.18\%$; (b) $H_u = 16.53$ m, void fraction of air pocket $\alpha = 0.07\%$

is located upstream of the ball valve. While the initial void fraction of the air pocket is close to 0, the maximum heads of PT1 and PT2 decrease and both are close to that of PT5. This is because when the initial void fraction of the air pocket is small, both the air cushioning effect and water impact force are also small.

As shown in Fig. 5, the experimental investigation indicates that, under the constant inlet pressure, as the initial void fraction of the air pocket, α, becomes smaller, the maximum pressure of the air pocket increases at the beginning because the air cushioning effect is dominant and gradually reduced; then, the maximum pressure of air pocket obtains its highest value because the water impact force is gradually more dominant when the initial void fraction of the air pocket reaches a specific value (in this experiment, $\alpha = 6.18\%$). Subsequently, because the effects of air cushioning and water impact force are both reduced (practically negligible), the maximum pressure of the air pocket decreases with the decrease of α. Meanwhile, the time duration to get the maximum pressure becomes shorter with the decrease of the initial void fraction of the air pocket.

As aforementioned, Zhou (2000), Zhou et al. (2002), Lee and Martin (1999), and Lee (2005) concluded that "the maximum peak pressure of air pocket increases with the decrease of the initial void fraction of air pocket," based on their experiments with a higher initial void fraction of air pockets ($\alpha > 5.8\%$). Physically, the large air pocket entrapped in the confined pipe systems is similar to an accumulator that prevents high pressure from being generated, and the cushioning effect is more obvious with the larger air pocket. Thus, Lee (2005) and Zhou (2002) drew the preceding conclusion about the large air pocket. However, when the initial air pocket is small, especially when α is close to zero, the peak pressure is almost the same as a pure water hammer with no air; the water

J. Hydraul. Eng. 2011.137:1686-1692.

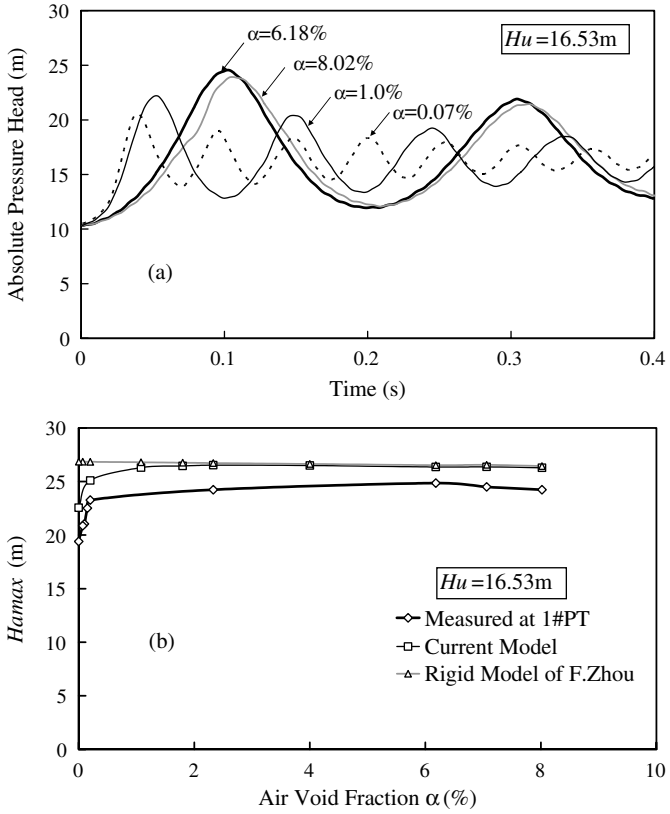

Fig. 5. Effects of the void fraction of air pocket on the pressure of the air pocket: (a) pressure oscillation pattern recorded by PT1; (b) change of the maximum pressure of the air pocket

impact force becomes gradually dominant with the increase of the air void fraction, which is demonstrated by the previously discussed experimental results. Therefore, the current experimental investigations are complementary to the preceding ones. The influence of the air pocket on the peak pressure can be summarized as follows: under a higher initial void fraction of the air pocket, owing to the decrease of the air cushioning effect, the maximum peak pressure of the air pocket becomes greater as α diminishes; when α reaches a certain small value, the smaller space for the water movement leads to the decrease in the water impact force, and thus the maximum pressure decreases as α becomes smaller.

Mathematical Model Verification

Compared with the complete elastic water model, the proposed model is introduced with a simplification to avoid the interpolations. The length range of ΔLw_i is the key of the current model and affects the calculated accuracy. Lee (2005) developed a complete elastic water model with an instantaneous open valve and a horizontal pipe (Lee's model). The parameter values used in Lee's calculations (2005) were as follows: pipe diameter $D = 0.026$ m, pipe length $L = 10.4$ m, water density $\rho = 1{,}000$ kg/m^3, wave speed $a = 600$ m/s, $f = 0.025$, air polytropic exponent recommended $m = 1.4$, initial pressure of air pocket $H_{a0} = 1.0 \times 10^5$ Pa (10.2 mH_2O). The case with $H_u = 40.8$ m, $\alpha = 44.81\%$, and $\Delta x = 0.01$ m is simulated with both the current model and Lee's elastic model. The length range of ΔLw_i in the current model is assumed to be $N\Delta x \le \Delta Lw_i < (N+1)\Delta x$. Fig. 6 shows the results of different length ranges of ΔLw_i (different N values), and the smaller ΔLw_i is, the closer the calculated result is

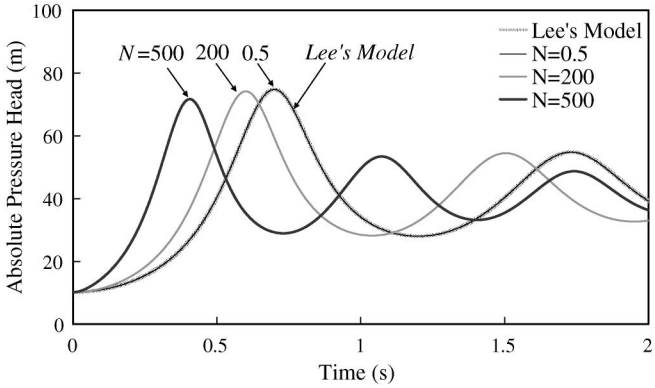

Fig. 6. Comparison of the current model and Lee's elastic model

to Lee's model. The current model with $0.5\Delta x \le \Delta Lw_i < 1.5\Delta x$ can achieve the consistent air pressure oscillation pattern with Lee's elastic model.

The mathematical model developed here can be also applied for an undulated pipeline system in which the valve opening time is taken into account. The wave speed, friction factor, the minor losses at the ball valve, and the valve opening time measured from the experiments are used as input parameters in the modeling.

Fig. 7 compares the computed and measured pressure oscillation patterns. Fig. 7(a) compares a horizontal pipe containing an entrapped air pocket. The measured data and rigid model result are abstracted from Zhou's doctorial dissertation (Zhou 2000), which considers the variable length of water columns. Fig. 7(b) compares the undulated pipeline discussed here. These comparisons demonstrate that the proposed model provides improved

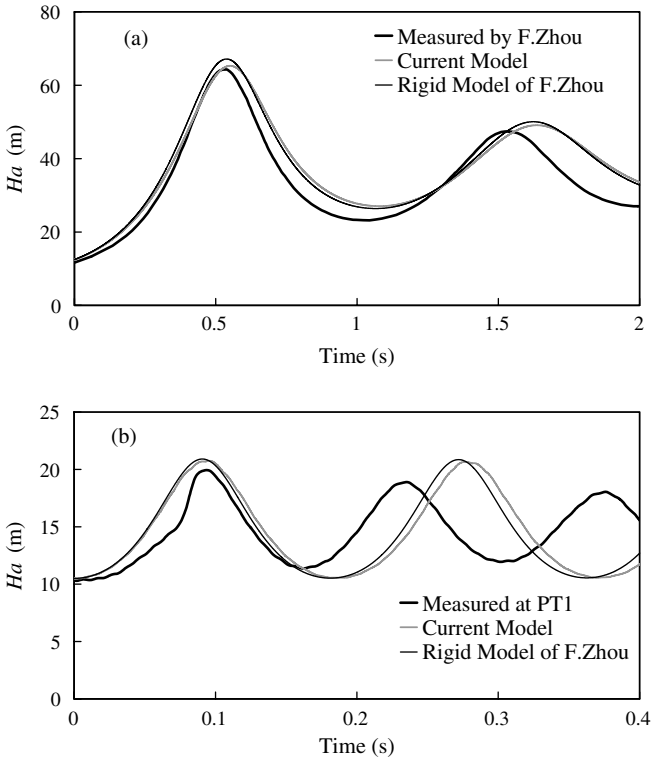

Fig. 7. Comparisons between calculated and experimental pressure oscillation pattern: (a) horizontal pipeline [Zhou's experiment (2000)]; (b) undulated pipeline (current experiment, $\alpha = 1.08\%$, $Hu = 15.26$ m)

J. Hydraul. Eng. 2011.137:1686-1692.

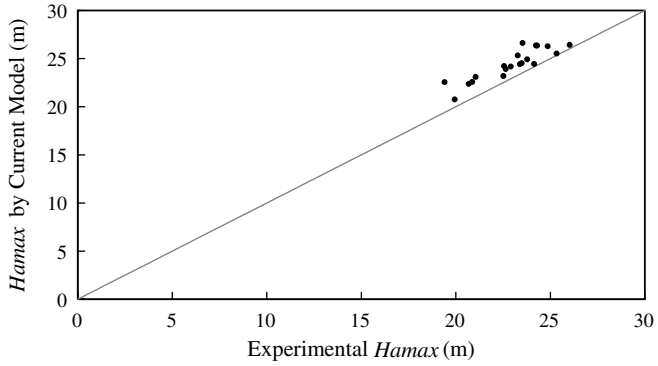

Fig. 8. Comparison between computed and measured maximum pressures

(more accurate) predictions for both horizontal and undulated pipelines.

Fig. 5(b) shows that as the initial void fraction of air pocket increases, the results from both elastic and rigid models are generally consistent, and both are slightly higher than the experimental pressures. However, the difference from both models becomes progressively more significant with the decrease in the initial void fraction of the air pocket. The results from the currently proposed model demonstrate that the maximum peak pressure increases slowly at beginning and then decreases rapidly with the decrease of the initial void fraction of air pocket, which has the same law as the measured result; whereas the results from the rigid model of Zhou shows that the maximum peak pressure proportionally increases with the decrease of the initial void fraction of the air pocket. Thus, the rigid model is either highly conservative or entirely unsuitable for predicting the pressure when smaller initial void fractions are considered.

Fig. 8 compared the computed and observed peak pressures. To further verify the proposed model using the experimental measurement, the numerical modeling and experiment are repeated by changing the inlet pressure and initial void fraction of the air pocket, and a simple statistical analysis is conducted by defining a relative error:

$$\varepsilon = \frac{|H_{\text{exp}} - H_{\text{calc}}|}{H_{\text{calc}}} \tag{10}$$

The average error is found to be 5.99%, the maximum error is 13.95%, and the minimum 0.78%. The error is less than 10% for 90% of the tests. This finding demonstrates that the current model practically quantifies pressure oscillation, especially for the (usually most severe) first cycle of oscillation.

The preceding comparisons and analyses indicate that the peak pressure predicted by the currently proposed model tends to be conservative from a design perspective, because it is slightly higher than the experimental value. Compared with the measurements, the attenuation of the calculated pressure curve after the first peak is slower and the cycle is longer. Possible reasons for these differences include (1) using the steady-flow friction factor for the unsteady flow would underestimate the pressure wave attenuation at moderate and high frequencies (Chaudhry 1985); (2) the air phase is treated as an adiabatic process with a constant polytropic exponent m ($m = 1.4$), whereas the true dynamic involves a complicated heat transfer process (Graze 1996); (3) the integrality of the entrapped air pocket that is assumed throughout the transient process might actually be broken up by the filling water, especially after the first compression of the air pocket; (4) the flow transients in the elbow part of the undulated pipeline are complicated, and the energy loss is also difficult to be quantify. Therefore, if the friction factor and characteristics of the air pocket were described more accurately, the proposed model would presumably be able to more successfully predict for the pressure oscillation pattern; in practice, such a search for a further improved model would seldom be economically justified.

Conclusions and Discussions

The observation from these physical experiments reveals the effect of the entrapped air pocket on the flow transients during the pipeline filling. Keeping both pipe length and inlet pressure constant, the maximum peak pressure of the air pocket increases at first and then decreases with the reduction of the void fraction of air pocket. The highest pressure occurs at a smaller void fraction of the air pocket (at $\alpha = 6.18\%$ in the previously discussed case study). The pressure change law found in this paper is not incompatible with the conclusions made by Zhou (2000), Zhou et al. (2002), Lee and Martin (1999), and Lee (2005), that is, "the maximum peak pressure of air pocket increases with the decrease of the initial void fraction of air pocket," but their experiments were conducted for a higher initial void fraction of the air pocket (not less than 5.8%) in a horizontal pipe. In sum, the current research is not only consistent with the conclusion of Zhou and Lee, but also complementary for the investigation on the influence of the void fraction of the air pocket on the transient pressure during pipe filling.

The proposed model makes a reasonable simplification to capture the air-water interface; the resulting simulations not only hold the same accuracy with the complete elastic water model, but also avoid the interpolation complexity. In addition, the model considers many potentially important factors, such as elevation change of the pipeline and valve opening time. Although some unavoidable assumptions and limits of the numerical model resulted in differences between the calculated and measured results, the maximum peak pressure from the proposed model is closer to experimental measurements than the rigid water model. For variations of the void fraction of the air pocket, the prediction of the current model provides the same pattern of the maximum peak pressure as from the experimental observation. However, the rigid water model cannot easily predict the peak pressure and can even result in an opposite peak pressure variation pattern when the void fraction of the air pocket is sufficiently small.

Acknowledgments

The authors gratefully acknowledge the financial support on this research from the National Natural Science Foundation of China (Grant No. 50979029).

Notation

The following symbols are used in this paper:

A = section area of pipe;
a = wave speed;
C^-, C^+ = name of characteristic equations;
D = diameter of pipe;
f = friction coefficient;
g = gravitational acceleration (9.81 m/s^2);
H = instantaneous piezometric head;
H_a = air pressure head (absolute value);
H_{a0} = initial air pressure head (absolute value);
H_{amax} = the maximum air pressure head (absolute value);

J. Hydraul. Eng. 2011.137:1686-1692.

H_{calc} = calculated value of the maximum absolute air pressure;
H_{exp} = calculated value of the maximum absolute air pressure;
H_P = piezometric head at node;
H_r = upstream water head (relative value);
H_u = upstream water head (absolute value);
L = length of pipe;
L_a = length of air pocket;
L_{a0} = initial length of air pocket;
L_{va} = the distance between valve and air-water interface;
m = polytropic exponent;
Q = flow rate;
Q_P = flow rate at node;
V_a = air volume;
V_{a0} = initial air volume;
x_w = location of air-water interface;
Z_C = elevation of pipe center of air-water interface;
α = initial void fraction of air pocket (initial air volume to total volume of air and water);
ΔLw_i = distance from air-water interface to point nearby the interface;
Δt = time step;
Δx = grid length;
ξ = relative error of calculation;
ξ_j = minor loss coefficient of the inlet; and
ρ = water density.

References

Cabrera, E., Abreu, J., Perez, R., and Vela, A. (1992). "Influence of liquid length variation in hydraulic transients." *J. Hydraul. Eng.*, 118(12), 1639–1650.

Chaudhry, M. H. (1985). "Limitation of hydraulic-transient computation." *21st IAHR Congress*, Int. Association for Hydraulic Research, Madrid, Spain, 132–136.

De Martino, G., Fontana, N., and Giugni, M. (2008). "Transient flow caused by air expulsion through an orifice." *J. Hydraul. Eng.*, 134(9), 1395–1399.

Environmental Hydraulics Group (EHG). (1996). "Hydraulic transient evaluation of the City of Edmonton sewerage system, Phase I." *Research Rep.*, EHG, Ontario, Canada.

Graze, H. R. (1996). "Thermodynamic behavior of entrapped air in an air chamber." *7th Int. Conf. on Pressure Surges*, BHR Group, Bedfordshire, UK, 549–560.

Guo, Q. Z., and Song, C. C. S. (1990). "Surging in urban storm drainage systems." *J. Hydraul. Eng.*, 116(12), 1523–1537.

Lee, N. H. (2005). "Effect of pressurization and expulsion of entrapped air in pipelines." Doctoral dissertation, Georgia Institute of Technology, Atlanta.

Lee, N. H., and Martin, C. S. (1999). "Experimental and analytical investigation of entrapped air in a horizontal pipe." *Proc., 3rd ASME/JSME Joint Fluids Engineering Conf.*, ASME, New York, 1–8.

Liu, D. Y., and Suo, L. S. (2004). "Rigid model for transient flow in pressurized pipe system containing trapped air mass." *Adv. Water Sci.*, 16(6), 717–721 (in Chinese).

Liu, D. Y., and Zhou, L. (2009). "Numerical simulation of transient flow in pressurized water pipeline with trapped air mass." *2009 Asia-Pacific Power and Energy Engineering Conf. (Appeec)*, IEEE Power and Energy Society, New York, 104–107.

Martin, C. S. (1976). "Entrapped air in pipelines." *Proc., 2nd Int. Conf. on Pressure Surges*, British Hydromechanics Research Association, Bedford, UK, 15–27.

Ocasio, J. A. (1976). "Pressure surging associated with pressurization of pipelines containing entrapped air." *Special M. S. Research Rep.*, School of Civil Engineering, Georgia Institute of Technology, Atlanta.

Wylie, E. B., and Streeter, V. L. (1993). *Fluid transients in systems*, Prentice Hall, New York.

Zhou, F. (2000). "Effects of trapped air on flow transients in rapidly filling sewers." Doctoral dissertation, University of Alberta, Alberta, Canada.

Zhou, F., Hicks, F. E., and Steffler, P. M. (2002). "Transient flow in a rapidly filling horizontal pipe containing trapped air." *J. Hydraul. Eng.*, 128(6), 625–634.

Zhou, L., Liu, D. Y., and Ou, C. Q. (2011). "Simulation of flow transients in a water filling pipe containing entrapped air pocket with VOF model." *Engineering Applications of Computational Fluid Mechanics*, 5(1), 127–140.

J. Hydraul. Eng. 2011.137:1686-1692.